2021

The effect of photobiomodulation on cerebral blood flow

BOSTON UNIVERSITY

COLLEGE OF ENGINEERING

Thesis

THE EFFECT OF PHOTOBIOMODULATION ON CEREBRAL BLOOD FLOW

by

MARIA IENNACO

B.S., Boston University, 2019
B.A., Boston University, 2019

Submitted in partial fulfillment of the

requirements for the degree of

Master of Science

2021

Approved by

First Reader

David A. Boas, PhD
Professor of Biomedical Engineering
Professor of Electrical and Computer Engineering

Second Reader

Xue Han, PhD
Associate Professor of Biomedical Engineering

Third Reader

Anna Devor, PhD
Associate Professor of Biomedical Engineering

Dedication

To my mom and dad, who patiently helped me understand fractions in elementary school, never missed a gymnastics competition, and sat through practice presentations from “The Parts of a Cell” in fourth grade to my thesis defense now. You are my greatest inspirations and supporters, thank you for your endless encouragement.

To my nana, who touched countless lives as a nurse and taught all of her grandchildren that they can do anything they set their mind to. Thank you for believing in me always.

Acknowledgments

I am incredibly grateful for all of the support I have received in producing this work.

I would first like to thank my advisor, Professor David Boas, who provided invaluable guidance in formulating the research questions and approach. His constant support and feedback were instrumental in the success of the thesis. He challenges and inspires me to constantly improve as a scientist and I am deeply appreciative to have the opportunity to work in his lab.

I would also like to express my sincere gratitude to Professor Xue Han and Professor Anna Devor. They both provided valuable insight and lively discussions throughout the course of this research that constantly motivated me to dive deeper into the data and learn more.

Finally, I would like to thank all of the members of the BOAS Lab for welcoming me into such a supportive, collaborative environment. I would especially like to thank Smrithi Sunil, Jack Giblin, Jiarui Yang, and Jianbo Tang for their expertise, patience, and willingness to help guide and teach me. I have learned so much from everyone at the lab and am honored to have worked alongside them.

THE EFFECT OF PHOTOBIOMODULATION ON CEREBRAL BLOOD FLOW

MARIA IENNACO

ABSTRACT

Photobiomodulation (PBM) therapy involves the irradiation of tissues with red to near-infrared (NIR) light at low power densities to stimulate healing, reduce inflammation, and promote optimal cellular functioning. These beneficial effects are thought to occur due to the absorption of NIR light by the chromophore, and terminal enzyme in the mitochondrial electron transport chain, cytochrome c oxidase (CCO). It is hypothesized that increased oxygen consumption due to the photostimulation of CCO, as well as photodissociation of the vasodilator nitric oxide from its binding site in the binuclear center of CCO, contribute to improved tissue healing by increasing blood flow to the irradiated region. Applied to the brain, PBM therapy has the potential to improve many neurological injuries and diseases for which reduced cerebral blood flow (CBF) is a common finding. This study examines whether cortical irradiation with NIR light has an impact on CBF in mice. Mice were administered brain PBM via 810nm, 190mW LED for 18 minutes. CBF was measured before, during, and after treatment using Doppler Optical Coherence Tomography. Results from 16 trials demonstrated a significant, 40% increase in CBF during NIR treatment. This CBF increase was not observed during control trials. Additionally, irradiation with a 730nm LED did not increase CBF, indicating that the blood flow increase observed with 810nm irradiation was not simply due to tissue heating. These findings provide support for the value of PBM therapy for the treatment of neurological conditions.

Contents

List of Tables

List of Figures

List of Abbreviations

ATP	.....	Adenosine Triphosphate
BA	.....	Basilar Artery
CBF	.....	Cerebral Blood Flow
CCO	.....	Cytochrome C Oxidase
DOCT	.....	Doppler Optical Coherence Tomography
ETC	.....	Electron Transport Chain
Hb	.....	Deoxyhemoglobin
HbO	.....	Oxyhemoglobin
LED	.....	Light Emitting Diode
MCA	.....	Middle Cerebral Artery
NIR	.....	Near-Infrared
NO	.....	Nitric Oxide
OCT	.....	Optical Coherence Tomography
OCTA	.....	Optical Coherence Tomography Angiography
PBM	.....	Photobiomodulation
ROI	.....	Region of Interest
TBI	.....	Traumatic Brain Injury

Chapter 1

Introduction

1.1 Review of Photobiomodulation

Photobiomodulation (PBM) therapy involves irradiating tissue with red to Near-Infrared (NIR) light at low power densities to stimulate healing and promote optimal cellular functioning. The therapeutic effect was accidentally discovered in 1967 when Dr. Endre Mester attempted to use a ruby laser to destroy a tumor that had been implanted in a rat. The laser was significantly lower powered than lasers used in similar studies and instead of destroying the tumor, the wound around the tumor was rapidly healed and hair growth was stimulated in the irradiated area (Mester et al., 1968; Kovács, 1974). Since then, this therapy has been shown to be beneficial in treating a wide range of health conditions throughout the body; from stimulating rapid wound healing (Minatel et al., 2009; Schubert, 2001) and relieving acute and chronic pain (Chow et al., 2010; Chow et al., 2006) to improving visual acuity in retinal diseases (Ivandic and Ivandic, 2008). PBM has even been proposed as an adjunctive treatment for COVID-19 due to its known anti-inflammatory effects in lungs (Nejatifard et al., 2021; de Lima et al., 2010). Most recently, PBM research has expanded to examine its effects on cortical tissue in neurological conditions like Stroke, Traumatic Brain Injury, and Alzheimer's Disease. By irradiating the cortex (transcranially in humans) PBM therapy has the potential to treat a wide array of neurological conditions that otherwise have few, if any, effective treatments.

While the precise mechanism of PBM is debated, it is widely agreed that the beneficial effects are due to the photostimulation of mitochondria through the chromophore

cytochrome c oxidase (CCO), which is complex IV in the mitochondrial electron transport chain (ETC). CCO has absorption peaks at 605, 620, 655, 680, 760, and 830nm, which coincide with the action spectra of PBM (Karu and Kolyakov, 2005; Ball et al., 2011). These peaks conveniently fall within the tissue "optical window" for which absorption by water and the other major chromophores in tissue (hemoglobin and melanin) are minimized, allowing for increased tissue penetration of light (Chung et al., 2012). When tissue is exposed to these wavelengths of light, there are well documented increases in mitochondrial membrane potential, and levels of ATP, cAMP and Nitric Oxide (NO) (Hamblin and Huang, 2019). This evidence of increased mitochondrial function further supports the theory that CCO underlies the beneficial effects of PBM. The mitochondrial stimulation triggers a cascade of molecular events resulting in; activation of transcription factors important for cell survival, such as NF-κB (Chen et al., 2011), downregulation of pro-apoptotic factors (Yip et al., 2011), and modulation of pro and anti-inflammatory cytokines (de Freitas and Hamblin, 2016). These downstream changes explain the long-lasting beneficial effects that are observed in patients, after even just a single exposure to NIR light.

Close attention must be paid to the PBM parameters used to ensure that a sufficient dose of NIR light reaches the targeted tissue to produce a biological effect. This is complicated by the large number of treatment variables, of which slight alterations can completely change outcomes. A recent review of these complexities listed common factors shown to affect PBM success including, "wavelength, energy density, power density, total energy, total power, pulse structure, spot size, tissue absorption characteristics, and treatment repetition" (Zein et al., 2018). Wavelength is the most widely agreed upon setting. PBM studies typically employ red light in the 620-700nm range or NIR light in the 780-1100nm range, with longer wavelengths favored for deeper tissue penetration (Chung, 2012). Light power must be low to avoid tissue heating and damage, and is typically used in the range of 1-1000mW (Chung, 2012). Optimal energy density and power density settings are much

more elusive. Energy density or fluence is defined as the amount of light energy delivered per unit area and is often thought of as the "dose" in PBM therapy. Power Density or irradiance is the amount of power delivered per unit area. Multiplying the irradiance in units of mW/cm2 by the irradiation time in seconds yields the fluence with units of J/cm2. Therefore, increasing irradiation time while maintaining the same light power and spot size, increases the fluence or "dose" of PBM. A fluence range of 3-10 J/cm2 is generally accepted as an adequate dose to stimulate metabolic activity (Zein et al., 2018). A search of the literature reveals an overwhelming amount of different combinations of settings used for the numerous parameters. A summary of these parameters for all known in vivo stroke PBM studies are listed in the appendix. These uncertainties have limited progress in the field.

1.2 Photobiomodulation in the Brain

PBM creates an optimal environment for healing by; stimulating blood flow, promoting cell-survival and regeneration, and decreasing harmful inflammatory responses. These effects make the therapy well suited for treating neurological conditions. However, progress has been somewhat limited due to inconsistent findings. For example, researchers demonstrated that a single, 2-minute application of 808nm laser applied transcranially to rats, 24 hours after experimentally induced stroke, was able to improve neurological deficits measured at 14, 21, and 28 days post-stroke (DeTaboada et al., 2006). A second study with the same protocol demonstrated this improvement in neurological outcome as well, and immunohistochemical staining revealed evidence of increased neurogenesis (Oron et al., 2006). A third study of PBM in a rabbit model of embolic stroke, reported improved behavioral outcome and increased cortical ATP content compared to sham-PBM and even in healthy, untreated controls (Lapchak et al., 2007 and 2010). Large clinical trials were then initiated, known as the "Neurothera Effectiveness and Safety Trials" (NEST-1, NEST-

2, and NEST-3), in which a single treatment of 810nm laser was applied to the head of ischemic stroke patients within 24 hours post-stroke. NEST-1 and NEST-2, with 120 and 660 patients respectively, found significantly improved neurological outcome via the NIH Stroke Severity Scale in laser treated patients compared to sham, and this improvement was still evident at 90 days post-stroke in 70% of patients (Lampl et al., 2007; Zivin et al., 2009). However, NEST-3, which was planned to involve 1000 patients, was halted midway due to a lack of statistical significance (Hacke et al., 2014). The failure of NEST-3 may have been due to variations in time between stroke and treatment application as well as a lack of consideration for stroke location and depth. The failure of the NEST-3 trial has cast some doubt on brain PBM, however a large body of behavioral and molecular evidence shows that if light and treatment parameters are optimized, NIR light therapy can be quite effective in treating a variety of neurological conditions.

One compelling indication of the value this therapy could have in neurological settings is the finding that PBM application throughout the body improves blood flow (Frangez et al., 2017; Podogrodzki et al., 2016). This is thought to be a direct result of the previously discussed CCO absorption of NIR light. It is theorized that NIR light causes photodissociation of the powerful vasodilator NO from the binuclear center (a3/CuB) of CCO. The dissociation of inhibitory NO from the ETC increases CCO activity and therefore oxygen consumption. (Salehpour et al., 2018). The resulting increased need for oxygen as well as vasodilation due to NO, stimulates increased blood flow. Several studies have provided support for these theories. In a 2016 study, researchers applied a 1065nm laser to the forearms of healthy participants and used broadband near-infrared spectroscopy to measure significant increases in CCO and oxygenated hemoglobin concentrations (Δ[CCO] and Δ[HbO], respectively) in laser treated groups compared to placebo. This Δ[CCO] preceded and was linearly related to Δ[HbO], indicating that NIR light stimulates CCO and increases oxygen consumption. (Wang et al., 2016). In another study, researchers irradiated mouse primary

cortical neurons with an 810 nm laser and measured resulting increases in NO levels using fluorescent probes. (Sharma et al., 2011). These findings provide molecular evidence for the mechanism of PBM-induced blood flow increase.

Chapter 2

Quantification of Cerebral Blood Flow

2.1 Previous Studies of CBF during PBM

Since a common finding in nearly all neurological injuries and diseases is reduced cerebral blood flow (CBF) (Sweeney et al., 2018), a demonstration of increased CBF resulting from PBM would provide strong support for the value of this therapy. Many studies have demonstrated improved behavioral outcomes of brain PBM in conditions like stroke, TBI, and depression in both animals and humans (Salehour et al., 2018). Research has also examined cellular and neurochemical changes resulting from PBM (Lee et al., 2016). However, few have closely examined neurovascular changes that underlie this improved outcome.

A study by Uozumi et al. in 2010 irradiated the exposed skull of healthy, anesthetized mice with an 810nm laser for 45 minutes with a 3mm diameter exposure field. They semi-quantitatively measured CBF by using a laser Doppler blood perfusion imager to create color images of blood perfusion in the area before and at 15, 30, and 45 minutes during laser treatment. Using power densities of 0.8, 1.6, and 3.2 W/cm^2 they found that blood flow increased by 9.1%, 30.4%, and 30.5% respectively compared to the sham group. They concluded that this was not due to a heating effect by measuring temperature of the tissue with a thermocouple near the irradiation area and finding it only increased by about 0.8°C during 30 minutes of the 1.6W/cm^2 irradiation. However, they noted that for the 3.2W/cm^2, mean temperature rise during 45 minutes was 3.8°C. The group also used an amperometric NO-selective electrode to measure nitric oxide in the brain during 1.6W/cm^2 and found an immediate increase in NO concentration when the laser was turned on that returned to base-

line immediately after the laser was turned off. NO concentration in the sham control mice remained unchanged. They further examined whether 30min of 1.6W/cm^2, 810nm laser before bilateral common carotid artery occlusion (BCCAO) would improve CBF, finding that pretreatment suppressed the reduction in CBF from 30 seconds to 15 minutes after the start of BCCAO (Uozumi et al., 2010). This study was an impressive example of changes that occur in the brain during PBM, however the blood flow measurements were "semi-qualitative" and researchers noted that the measurement technique used in the BCCAO analysis was not reliable for distinguishing low blood flow. Furthermore, in their healthy PBM study, CBF changes were only recorded at three time points, 15, 30, and 45 minutes, after the start of irradiation.

There have also been a few studies measuring PBM-induced CBF changes in humans. In 2014 Salgado et al. administered transcranial LED therapy to elderly women with a 627nm LED to four points on frontal and parietal regions for 30 seconds on each point, twice per week for 4 weeks (0.2W power, 70mW/cm^2 power density, 10 J/cm^2 energy density, 13mm spot size). Blood flow velocities of the bilateral middle cerebral arteries (MCA) and the basilar artery (BA) were measured via transcranial Doppler ultrasound once before the first LED treatment and once four weeks later, after the last treatment. Increases in systolic and diastolic velocity in the left MCA (25% and 30%, $p<0.005$) and BA (17% and 25%, $p<0.03$) were reported although the right MCA did not show a statistically significant increase (Salgado et al., 2014). This finding that transcranial LED alters blood flow in elderly women substantiates the claim that PBM could be useful for treating a wide range of neurological conditions exhibiting decreased blood flow as a symptom. However, this study only examined blood flow changes at two time points four weeks apart and measurements were limited to three main arteries.

2.2 Aims of this Study

Research on PBM-induced CBF changes have mainly examined broad, relative (not quantitative) blood flow changes. Furthermore, they only examined CBF at a few time points, typically just two points, one before PBM and one after completion of the entire treatment protocol (Salgado et al., 2014; Hipskind et al., 2019). No study has imaged the vasculature, examined detailed neurovascular changes, or closely analyzed the time course of these changes before, at many points during, and after photobiomodulation in the brain. This study tests the hypothesis that brain PBM causes increased CBF, by imaging the cortex of mice with Doppler Optical Coherence Tomography (DOCT) before, during, and after PBM with 810nm LED. By employing DOCT, an absolute, quantitative measurement of blood flow and visualization of vasculature can be obtained with high spatial resolution in 3-D. This will allow for a close analysis of blood flow in individual vessels throughout the course of treatment. If CBF is increased, a visualization and absolute measure of this time course would be compelling evidence of the value of PBM for the treatment of neurological conditions involving reduced blood flow. Furthermore, examination of the time course may point to an optimal energy density (dose) of light that most efficiently increases CBF at this specific wavelength and power density. Since energy density increases with irradiation time for a given light power and spot size, analysis of blood flow over time may indicate a minimum threshold energy density required to stimulate increased CBF. It may also demonstrate a maximum energy density after which further CBF increase is not observed. This would be a valuable insight given the previously discussed uncertainties in the field over optimal PBM parameter settings.

Chapter 3

Methods

3.1 LED and PBM Parameter Selection Overview

Progress in brain photobiomodulation has been hindered by uncertainties over optimal irradiation parameters. With many parameters to vary, a wide range of power and energy densities investigated in different studies, occasionally incorrect or incomplete parameter reporting, and sometimes seemingly arbitrary power or duration settings used, this is an area that needs further investigation. See the appendix for insight into the complexity of parameter selection. Table 3.1 lists the LED and irradiation settings used for this study, procedures are described in depth in section 3.3.

Table 3.1: Relevant PBM Parameters used for Irradiation Procedures.

Procedure (Section Number)	**810nm PBM to Brain** (3.3.1)	**810nm 25% Power to Brain** (3.3.2)	**810nm to Back** (3.3.3)	**730nm to Brain** (3.3.4)
Wavelength (nm)	810	810	810	730
Power (mW)	190 ± 10	47.5 ± 2.5	190 ± 10	150 ± 7.9
Irradiation Area (cm^2)	0.785	0.785	0.785	0.785
Power Density (mW/cm^2)	268 ± 28.8	67 ± 7.2	268 ± 28.8	212 ± 22.5
Irradiation Duration (seconds)	1080	1080	1080	1080
Energy Density (J/cm^2)	289 ± 31	72 ± 7.7	289 ± 31	229 ± 24

3.2 Irradiation Procedures

The Boston University Institutional Animal Care and Use Committee approved all experimental procedures. Four wild type mice (male, C57BL/6J) were prepared with either a double crystal skull (n = 2, aged 14 months at the time of measurements) or a full crystal skull (n = 2, aged 7 months). Mice were allowed at least one month to recover from surgery. Since the mice would not be anesthetized during imaging, they were then trained daily for two weeks to acclimate them to the experimental setup. During training each mouse was placed in a fabric cradle with its head fixed in a head clamping device that attached to the crystal skull, and placed beneath the OCT. Training duration increased by 5-10 minutes each day until a full 60-minute training period (the same duration of experiments) was reached. After two, 60-minute head-fixed training sessions the animals were acclimated and ready for experiments.

3.3 Animal preparation

For all experimental (and training) procedures, mice were briefly anesthetized with isoflurane (3% induction) so they could be fixed in the head clamp. Once awake, an OCTA measurement was acquired of a 2mm x 2mm region and of the 600 x 600 μm region of interest (ROI). Care was taken to select an ROI with multiple penetrating vessels visible. The trial then began with DOCT measurements acquired every 3 minutes for 21 minutes for a total of 7 “Baseline” flow measurements. Immediately following the 7th baseline measurement, the LED was turned on to the appropriate power for the experiment (described below) and DOCT measurements continued every 3 minutes for 18 minutes (6 “PBM” flow measurements total). The LED was then immediately turned off and another 18 minutes of repeated DOCT measurements followed (6 “Recovery” flow measurements total). Altogether, one trial consisted of 19 measurements over 57 minutes. A visual representation of one trial is shown in Figure 3·1. Mice were then anesthetized again with isoflurane (3%

induction), removed from the head clamp and placed back in their housing.

Figure 3·1: Trial time course for all irradiation procedures (sections 3.3.1 – 3.3.4).

No more than one trial was performed each day for any given mouse to reduce the likelihood of CBF effects from one trial of PBM carrying over to the next PBM trial. LED power was measured immediately before the start of each trial by clamping a power sensor (Standard Photodiode Power Sensor, Thorlabs Inc., S121C) in the same location that the cranial window would be fixed in the head clamp, and then verified again after the trial immediately following the removal of the mouse.

3.3.1 Brain Photobiomodulation with 810nm LED

An 810 nm LED (Thorlabs Inc., M810L3) was chosen for photobiomodulation and the beam was collimated with a collimation adapter (Thorlabs Inc., SM2F32-B) to achieve a spot size diameter of 1.0 cm (measured at a distance of 8 cm) which was equivalent in size to the mouse cranial window. The 810 nm wavelength was selected as it corresponds to a CCO absorption peak, and is within the tissue optical window (between 600-1100 nm). The LED was angled towards the mouse cranial window such that the 0.785 cm^2 spot irradiated the entirety of the 0.785 cm^2 cranial window from a distance of 8cm. The maximum power achievable with this LED and irradiation geometry, 190 ± 10mW, was used. Power density was 268 ± 28.8 mW/cm^2. The mouse cortex was irradiated for 18 minutes (1080 seconds) producing a total Energy Density of 289 ± 31 J/cm^2.

3.3.2 Brain Photobiomodulation with 810nm LED at 25% Power

To test if CBF changes resulting from procedure 3.3.1 were due to NIR photons or simply a result of other experimental conditions or physiological responses, the same procedure was performed but with the LED power decreased to 25% of the 190mW power used in the first procedure. Without adequate power delivered to the tissue, a PBM effect was not expected. The 810 nm LED was again positioned at a distance of 8 cm from the cranial window and angled to fully irradiate the window. Power was 47.5 ± 2.5 mW with an irradiated area of 0.785 cm^2, a power density of 67 ± 7.2mW/cm^2 and an energy density of 72 ± 7.7J/cm^2.

3.3.3 Irradiation of Mouse Back with 810nm LED

To further test if CBF changes were due to irradiation of the brain and not a sensory response or natural physiological fluctuations, the 810nm LED was positioned to instead irradiate the mouse's back from a distance of 8 cm. Irradiation of tissue at a location away from the brain was not expected to produce a PBM effect of increased blood flow in cortical tissue. Power was 190 ± 10 mW with an irradiated area of 0.785cm^2, a power density of 268 ± 28.8 mW/cm2 and an energy density of 289 ± 31 J/cm^2.

3.3.4 Investigation of Temperature Rise and Blood Flow Response

In order to assess if tissue temperature rise was a potential contributor to observed blood flow changes, a 730 nm LED (Thorlabs Inc., M730L5) was acquired. 730 nm corresponds to a dip in the absorption spectrum of CCO in which no PBM effect is expected. Therefore, if any blood flow increase were to occur as a result of 730 nm irradiation, it may be due to tissue heating effects. Again using the collimation adapter to collimate the light, the maximum power achievable with the 730 nm LED was 150 mW. The LED spot size was 1 cm in diameter at the center focus with a wider diameter of 6 cm of significantly less intense light.

To ensure an equivalent tissue temperature rise with both LEDs, the absorption coefficient (μ_a) of each wavelength in cortical tissue was calculated according to:

$$\mu_a = \varepsilon_{HbO}[HbO] + \varepsilon_{Hb}[Hb] \tag{3.1}$$

Where ε_{HbO} and ε_{Hb} are the extinction coefficients of HbO and Hb, and [HbO] and [Hb] are the concentrations of HbO and Hb in the brain (60μM and 40μM, respectively). For the 730nm LED, $\mu_{a,730nm}$ is calculated to be 0.1899cm-1 (given ε_{HbO} = 510 $\frac{cm^{-1}}{mol/L}$ and ε_{Hb} = 1296.5 $\frac{cm^{-1}}{mol/L}$. While for the 810nm LED, $\mu_{a,810nm}$ is 0.1999cm^{-1} (with ε_{HbO} = 914.3 $\frac{cm^{-1}}{mol/L}$ and ε_{Hb} = 798.7 $\frac{cm^{-1}}{mol/L}$). This means there is a 0.01cm^{-1} difference, or 5% increase in the absorption coefficient at 810 nm compared to 730 nm. To produce a comparable temperature rise, the power of the 810 nm LED was decreased by 5% (i.e. 7.5 mW) from the power used for the 730nm LED. So, while trials with the 730 nm LED used a power of 150 mW, trials with the 810 nm LED used a power of 142.5mW.

3.4 OCT measurement

Blood flow images were acquired via Doppler OCT measurements with a Spectral Domain OCT system (1310nm center wavelength, Thorlabs Inc.). A 10x objective was used providing a lateral resolution of 3.5μm. The axial resolution was 2.6μm and imaging speed was 76,000 A-scans/s. The ROI imaged was 600μm x 600μm (400 x 400 pixels in X and Y). A total of 20 A-scans were acquired at each spatial location. One complete ROI measurement was acquired in approximately 156 seconds.

3.5 Image processing and analysis

The raw data was processed to generate a 3D dataset of blood velocity for each time point. Penetrating vessels to later analyze across all time points were selected by examining the velocity data at the first time point. For each penetrating vessel, the depth (z) at which that

vessel was most visible in the en face (x, y) plane was identified. This depth would then be used for calculating that blood vessel's flow at all time points. Each vessel's flow (in mm^3/s) was measured at each timepoint by calculating the sum of the axial velocity (vz) of all pixels that comprise the vessel (with vz 0.1 mm/s), and then multiplying that sum by the area of each pixel ($2.25x10^{-6}mm^2$/pixel for the 600μm x 600μm ROI with 400 x 400 pixels in x and y). The equation is below:

$$VesselFlow = \sum_{n=1}^{\#ofpixels} v_{z,n} \times (2.25 \cdot 10^{-6} mm^2)$$

One trial's complete dataset consisted of a flow measurement at each of the 19 time-points for every vessel visible in that trial's imaged ROI. Each vessel's baseline flow value was calculated by taking the mean of the first seven blood flow measurements of the vessel. Then, the blood flow change of the vessel was calculated for each timepoint (t = 1 to 19) according to:

$$RelativeChange(t) = \frac{VesselFlow(t) - BaselineFlow}{BaselineFlow} \times 100\% \tag{3.3}$$

This was repeated for every vessel in the ROI. The trial's overall CBF change for each timepoint was then calculated by taking the mean of all vessel's relative change (calculated in Eq 3.3) at that timepoint.

Chapter 4

Results

4.1 Brain Photobiomodulation with 810nm LED at 190mW Increased Cerebral Blood Flow

Irradiation with 810nm, 190mW light increased cerebral blood flow in all trials. As an example, the results of a single trial of PBM are shown in Figure 4·1. A total of 13 penetrating vessels (2 veins and 11 arteries) were visible in this trial's ROI (labeled in **??**(A)). Every vessel exhibited increased blood flow during the 810nm irradiation. For the first 3 minutes of PBM, this increase from mean baseline flow ranged from 47.1% (vessel 6) to 419.3% (vessel 7). This trial's overall CBF change at each timepoint (the mean blood flow change across all vessels at each timepoint) is shown in Figure 4·1(C). There was an immediate blood flow increase of 145.9% during the first PBM measurement. This initial spike in blood flow then diminished slightly to a blood flow increase of 60.1% at the third PBM measurement before remaining constant at an increase of 69% for the remainder of the 18-minute irradiation. When the LED was turned off, flow immediately decreased (although still elevated from baseline by 21.6% to 55.0% throughout the recovery period). The mean blood flow increase during LED irradiation was 86.8% which was statistically significant compared to baseline increase, $t(24) = -6.3$, $p<0.001$. Mean blood flow increase during recovery was 41.9%, which was significant compared to baseline increase, $t(24) = -2.3$, $p = 0.0329$, but not compared to increase during LED irradiation, $t(24) = -2.75$, $p = 0.0636$.

The result of all trials of PBM with the 810nm LED at 190mW power (n=16) is shown in Figure 4·2. Figure 4·2(A) was obtained by taking the mean across all trials of the blood

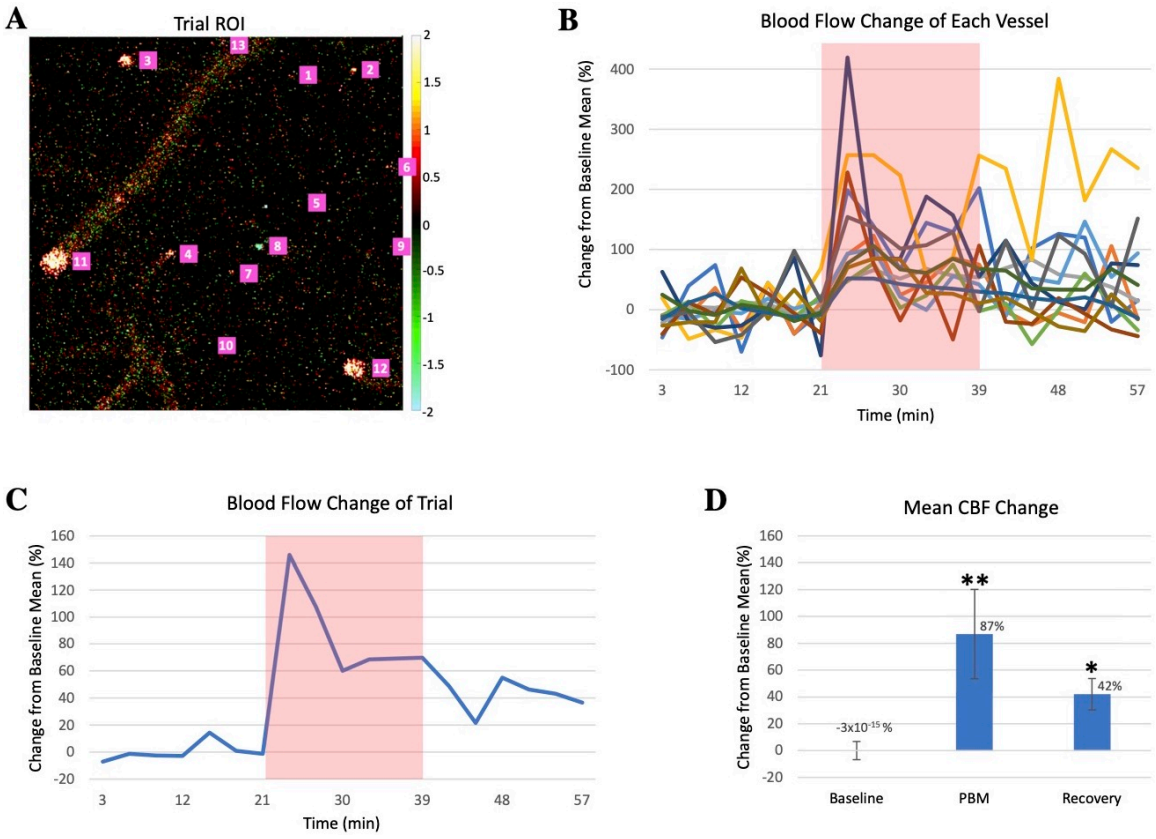

Figure 4·1: (A) DOCT blood flow image of trial ROI, en face (x,y) plane at depth z = 20. Penetrating vessels identified for blood flow analysis are labeled 1-13. Color bar: axial blood flow speed (mm/s); Positive value: blood flow towards brain surface; Negative value: blood flows into brain. (B) Blood flow change of each vessel over time, relative to mean baseline flow of respective vessel. (C) Overall blood flow change of all vessels in trial (average across all vessels at each time point). (D) Mean CBF change of each time period (Baseline, PBM, and Recovery) for trial. *p<0.05, **p<0.001. Pink shaded region in B and C indicates LED irradiation period.

flow change at each time point. Mean blood flow increase during LED irradiation was 40% which was statistically significant compared to baseline, t(30) = -5.17, $p < 0.001$. During recovery, mean blood flow increase was 20.7%, which was significant compared to baseline increase (t(30) = -4.29, $p < 0.001$), and compared to LED increase (t(30) = 2.12, p = 0.0425).

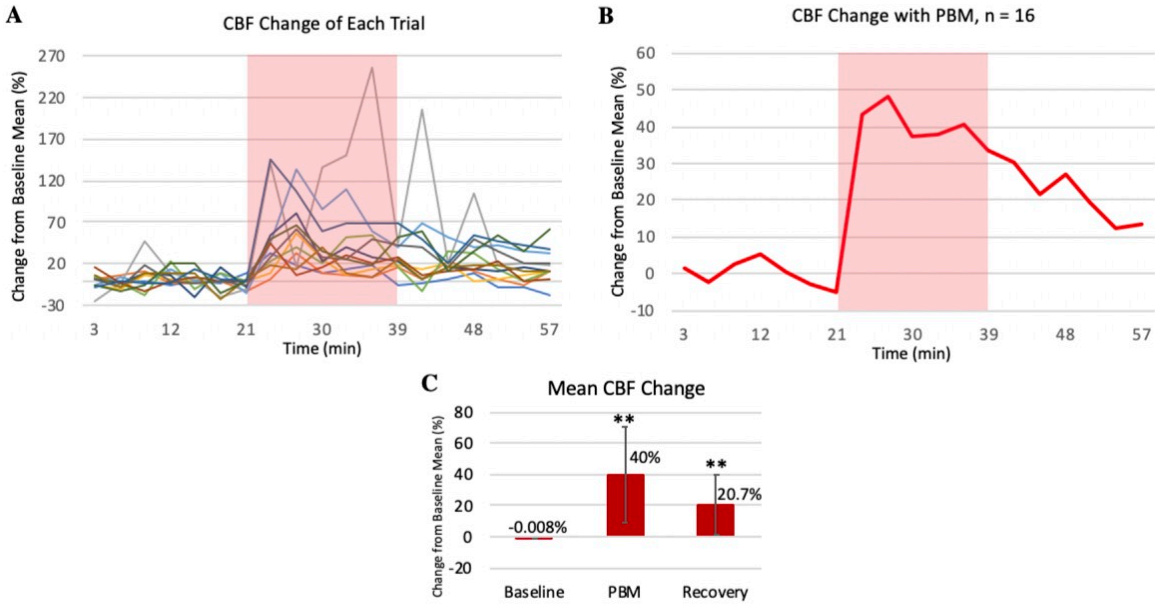

Figure 4·2: CBF change with 810nm, 190mW LED irradiation. (A) Overall CBF Change (average across all PBM trials at each time point, n = 16). (B) CBF change of each trial of PBM. (C) Mean CBF change for each period (Baseline, PBM, and Recovery) across all trials. **p<0.001. Pink shaded region in graphs indicates LED irradiation period.

4.2 Brain Irradiation with 810nm LED at 25% Power (47.5mW) did not Increase CBF

When irradiation power was decreased to 25% of the power used for PBM (from 190mW to 47.5mW) there was no evidence of significant blood flow change in any trial (n=3), as seen in Figure 4·3.

4.3 Irradiation of Back with 810nm LED at 190mW Power did not Increase CBF

When mice were irradiated with the 810nm LED at the same power settings as in section 4.1 but with the LED focused on their back instead of the brain, there was again no evidence of significant blood flow change in any trial (n=3). Figure 4·3 shows the blood flow change over time of these trials and the mean change across all trials.

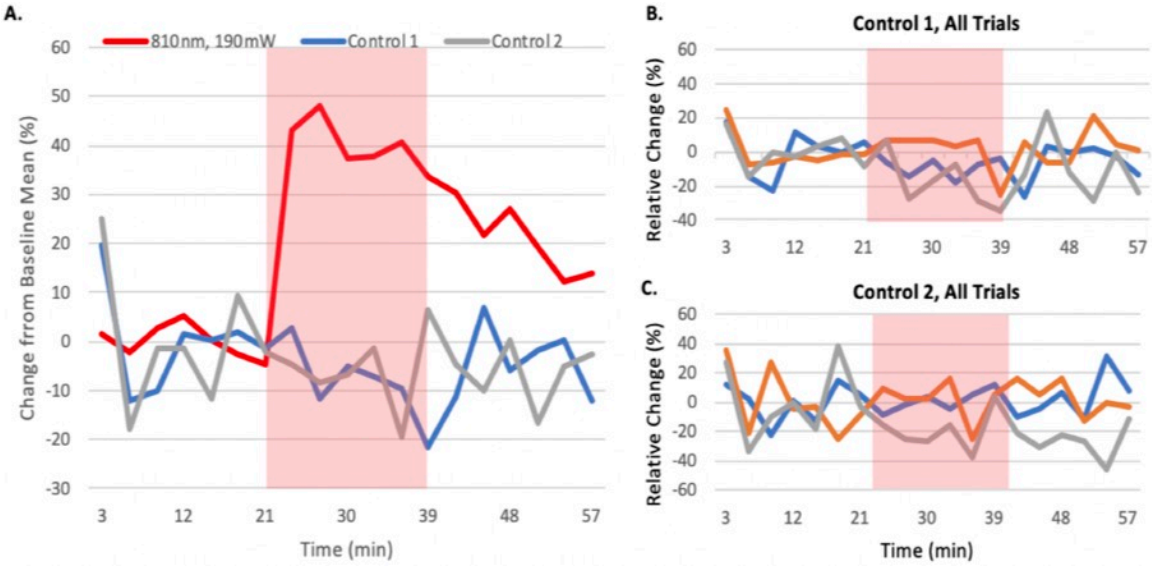

Figure 4·3: (A) CBF change of; 810nm, 190mW brain PBM trials (red line), Control 1 trials (blue line), and Control 2 trials (gray line). (B) CBF change of all Control 1 trials. (C) CBF change of all Control 2 trials. Pink shaded region in graphs indicates LED irradiation period. Control 1: 810nm, 25% power brain irradiation, n=3; Control 2: 810nm, 190mW LED to back, n = 3

4.4 Brain Irradiation with 730nm LED did not increase CBF while 810nm LED Irradiation with equivalent light absorption by tissue did

To test whether the effect seen in section 4.1 could have been related to tissue temperature rise and not true CCO-mediated PBM, the brain was irradiated with a 730nm LED at 150mW. Since there is no significant action of CCO at 730nm, if a blood flow increase was seen it could be attributed to temperature rise. Results are shown in Figure 4·4. There was no increase in blood flow seen with the 730nm LED in any trial (n=6). Instead, during irradiation blood flow decreased slightly to -8.5% of baseline, $t(10) = 3.38$, $p = 0.007$. Blood flow during recovery was also decreased to -9.39% of baseline, which was significant compared to Baseline ($t(10) = 2.89$, $p = 0.0168$), but not compared to LED irradiation ($t(10) = 0.224$, $p = 0.828$).

To invoke a similar temperature rise with 810nm irradiation, the 810nm LED was set to

142.5mW, a 5% lower power than the 730nm (because of a 5% increase in light absorption by tissue at 810nm). In contrast to the 730nm LED, the 810nm LED did correlate with significant increases in blood flow during irradiation (mean increase of 20% from baseline, t(2) = -17.3, p = 0.0033), and during recovery (mean increase of 17.1%, t(2) = -7.42, p = 0.0177 compared to baseline). Mean blood flow change during 810nm irradiation was significantly increased compared to blood flow change during 730nm irradiation, t(6) = -6.16, $p < 0.001$.

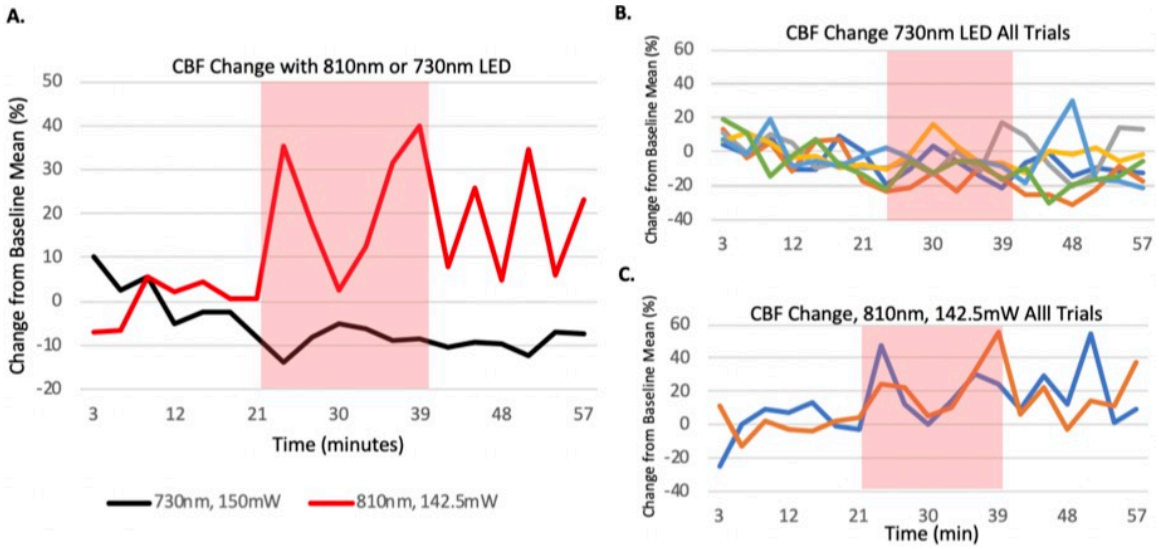

Figure 4·4: (A) CBF change of 730nm, 150mW trials (n = 6) and 810nm, 142.5mW trials (n = 2). (B) CBF change of all 730nm, 150mW trials. (C) CBF change of all 810nm, 142.5mW trials. Pink shaded region in graphs indicates LED irradiation period.

Chapter 5

Discussion

5.1 PBM with 810nm, 190mW light Increased CBF

Irradiation of the brain with an 810nm LED at a power density of 268 ± 28.8mW/cm2 correlated with an increase in blood flow in all trials (n=16), with a mean increase across trials of 40% compared to baseline, t(30) = -5.17, $p < 0.001$. This blood flow increase was immediate, occurring within the first 3-minute OCT measurement, and continuous, remaining elevated throughout irradiation. After the LED was turned off, the blood flow increase gradually diminished, yet still remained elevated above baseline for the rest of the trial.

The beneficial effects of brain PBM on functional outcome are well documented in the literature, for example improved neurological severity score after stroke or TBI in mice (Oron et al., 2006; Oron et al. 2007) and rabbits (Meyer et al., 2016), and improved executive functioning and neurological outcome in humans after Stroke (Lampl et al., 2007) or TBI (Naeser et al., 2011). Similarly, many studies have shown beneficial molecular changes resulting from brain PBM, for example suppression of neurotoxins and upregulation of growth factors in post-stroke rats (Leung et al., 2002), increased cortical ATP content in post-stroke rabbits (Lapchak et al., 2010), and decreased A plaques, amyloid load, and inflammatory markers in a mouse model of Alzheimer's Disease (DeTaboada et al., 2011). However there have been very few studies examining the effect of PBM on cerebral blood flow, this despite the fact that a decrease in CBF is an indication of nearly all neurological disorders.

The most widely cited evidence of increased CBF due to PBM is a 2010 study in which researchers used an 808nm laser to irradiate the brains of anesthetized mice for 45 minutes. CBF was measured semi-quantitatively using a laser Doppler blood perfusion imager before irradiation and at 15, 30, and 45 minutes during laser application. They found that at power densities of 800, 1600, and 3200 mW/cm2, CBF increased by 9.1%, 30.4%, and 30.5% respectively (Uozumi et. al., 2010). Our study built on this previous work by quantifying absolute blood flow in individual penetrating vessels and calculating a 40% increase in CBF beginning in just the first 3 minutes of PBM. Further, this increase was achieved using a significantly lower power density of 268 ± 28.8mW/cm^2.

The finding that blood flow is significantly increased within just 3 minutes of irradiation has implications for the usage of PBM in emergency care settings when time to treatment is crucial. For example, after ischemic stroke, PBM-induced CBF increase has the potential to preserve otherwise oxygen-deprived neurons and diminish neuronal death. NIR light therapy could also be valuable in the treatment of chronic neurological disorders that exhibit harmful CBF reduction; from conditions like Alzheimer's Disease and chronic TBI, to cognitive decline associated with normal aging.

While these findings add to the growing evidence of the value of PBM therapy for neurological disorders, a major question remains regarding the optimal parameters to use. The table in the appendix provides a glimpse into the complexities of establishing a single treatment protocol. In just stroke animal studies alone, researchers have measured positive neurological outcomes using power densities on the cortex ranging from 7.5mW/cm^2 (2 minutes, energy density 0.9 J/cm^2) (Lapchak et al., 2004) to 1100mW/cm^2 (30 minutes, energy density 19800 J/ cm^2) (Uozumi et al., 2010). The key to progressing the field of PBM may be understanding what causes one PBM protocol to be less effective or fail when seemingly very similar PBM protocols have impressive success. When comparing our study to the previous study of CBF in mice, it seems that the significantly higher power

used previously is unnecessary to produce an equivalent or even slightly larger effect in CBF.

It seems counterintuitive that a lower power treatment would have a larger effect on tissue, however it has been shown that the Bunsen-Roscoe law of reciprocity does not hold true for PBM outside of a certain (ill-defined) range of power densities. This law asserts that for photochemical reactions, the important parameter is only the number of photons absorbed. This would mean that two irradiation procedures with equal energy densities would have the same effect on tissue, even if one was a very low-power density for a long duration and the other a high-power density for a short duration. (Zein et al., 2018) This is not what is seen in PBM. Under a certain threshold power density, irradiation could continue for an infinite amount of time and no effect would be seen. Similarly, there is some upper limit of power density after which damaging photothermal effects occur. Instead, PBM seems to display a hormetic, or a biphasic dose response, in which there is some region where small to moderate doses of light elicit a beneficial effect, above this range larger doses inhibit the beneficial effects, and at some even higher dose threshold harmful effects are seen. This could explain why our study measured a slightly larger blood flow effect using a significantly lower power density than the study by Uozumi et al. There are a few other differences between this study and the previously described PBM study of CBF in mice. Uozumi et al irradiated the brain transcranially through the exposed skull (after a scalp incision) which would cause an attenuation of light reaching the brain and potentially decrease the effect of PBM. However, they estimated the power density of light transmitted to the brain to be 1100 and 2200 mW/cm2^2 for the 1600 and 3200 mW/cm^2 transcranial irradiation respectively. This is still a significantly higher power density than that used in our study. Another difference is the size of the irradiated area. Uozumi et al used a 3mm diameter exposure field on one hemisphere while our study irradiated the entirety of the 0.785cm^2 cranial window and therefore both hemispheres of the cortex. It

remains unclear to what extent these types of study-to-study differences in PBM parameters impact neurological outcomes. Establishing reliable, standard guidelines for each PBM parameter for a given health condition is of the utmost importance for progression and scientific acceptance of PBM therapy.

5.2 The Increased Blood Flow Effect is not due to other experimental conditions

Every effort was taken in each trial to eliminate any sensory stimuli that might cause functional activation and a blood flow response in the awake mice. Outside light and movement near the mouse was kept to a minimum throughout each trial and the only action taken during each trial was turning the dial of the power source to turn the LED on and off. The findings of Figure 4.3 strengthen the claim that the increased blood flow response was solely due to NIR irradiation and not other experimental conditions like fear-invoking stimuli, or residual effects of the anesthesia used briefly to place the mouse in the head clamp. When all experimental conditions remained constant but the LED illuminated a spot on the mouse's back rather than the cranial window, there was no blood flow change seen in any trial (n=3, Figure 4.4). Similarly, when the cranial window was illuminated with just 25% of the power used for PBM, 47.5mW (power density 72 ± 7.7mW/cm^2), no blood flow increase was evident.

It was hypothesized that a decreased power density would not provide the energy necessary to elicit a PBM response, however the choice of 25% of the original power was a slightly arbitrary decision. Interestingly, several studies, some of which are listed in the appendix, did report a response to PBM with power densities lower than the 72mW/cm^2 used here. There could be several reasons for this discrepancy including differences in animal models, outcome measures, and irradiation areas. Most notably, all of the studies in the appendix were in stroke models. It is possible that a lower dose of PBM is necessary to

see a response in a damaged brain than in a healthy brain. This is another demonstration of the need for further research on optimal parameters in different health conditions.

5.3 The Increased Blood Flow Effect is not due to tissue heating

Cortical tissue temperature rise due to photon absorption from 730nm, 150mW light was estimated to be equivalent to temperature increase from 810nm,142.5mW light. However, there is no CCO absorption band nor experimental evidence of CCO stimulation at 730nm, while stimulation by 810nm light has repeatedly been shown in the literature. Therefore, the significant increase in blood flow observed during 810nm, 142.5mW irradiation and recovery (20% and 17% respectively), combined with the complete lack of blood flow increase during 730nm, 150mW irradiation, indicates that CBF increases recorded in this study are likely a result of PBM and not due to a tissue heating effect.

Chapter 6

Conclusion

This study evaluated whether cortical irradiation with NIR light has an impact on cerebral blood flow in mice. Results from 16 trials of 810nm LED irradiation demonstrated a significant increase in CBF during both the treatment and recovery period. This CBF increase was not observed during control trials in which 810nm irradiation was applied sub-optimally for brain PBM, including; to the mouse's back instead of the brain (n = 3), or to the brain at 75% reduced power (n=3). Furthermore, 730nm LED irradiation showed entirely different results from the 810nm PBM trials, with mean blood flow actually decreasing throughout the trials (n=6). These results provide support for the potential value of NIR light therapy in the treatment of neurological conditions. Future work should further investigate the effect of NIR light on blood flow in diseased states, with a focus on unraveling the complexities of optimal PBM parameters. Photobiomodulation therapy has the potential to safely and non-invasively improve many devastating neurological and psychological conditions that currently have few effective treatments.

Appendix A

Previous PBM Stroke Studies

Table A.1 below lists a summary of parameters used in all known in vivo stroke studies of PBM. Parameters that were varied in each study are shaded either green, representing success, or red, representing failure, of that parameter in inducing beneficial effects. Bright green indicates the setting that performed the best of all successful settings in that study. The results column is shaded in cases where no parameters were varied. Empty table entries indicate the parameters were not listed in publication. An asterisk (*) indicates parameters that were not listed in the publication but were calculated for this study based on available data. Abbreviations: PW = pulsed wave, CW = continuous wave, MCAO = middle cerebral artery occlusion, RSCEM = Rabbit small clot embolic stroke, BCCAO = bilateral common carotid artery occlusion.

Study	Species	Stroke Model	Outcome Measures	Light Source	Power Density (mW/cm^2)	Time per treatment (min)	Energy Density (J/cm^2)	Pulse Structure	Time post-stroke (hours)	# of treat - ments	Results
Leung 2002[34]	Rat	MCAO (transient, 1hr)	Molecular	660nm Laser		1	2.64	PW 10kHz	0	1	Suppressed NOS activity (60% for setting 1, 86% for setting 2, 79% for setting 3), upregulated TGF-β1
						5	13.2				
						10	26.4				
Lapchak 2004[35]	Rabbit	Embolic stroke (RSCEM)	Behavioral	808nm Laser	25	10	15	CW	6	1	Improved clinical rating score, measured up to 21d, no benefit if applied 24h post-stroke
									1		
					7.5	2	0.9		3		
									24		
De Taboada 2006[17]	Rat	MCAO (permanent)	Behavioral	808nm Laser	7.5	2	0.9	CW	24	1	Improved neurological deficits measured at 14, 21, 28d post stroke
Oron 2006[18]	Rat	MCAO (permanent)	Behavioral	808nm Laser	7.5	2	0.9	CW	4	1	Improved neurological score up to 3wk later for 24h post stroke treatment but not 4h
									24		
							0.9	CW	24		Improved neurological function
								PW 70Hz			
Lapchak 2007[19]	Rabbit	RSCEM	Behavioral	808nm Laser	7.5	2	0.9	CW	12	1	PBM at 12h did not improve clinical rating score
								PW 1kHz			
					7.5	2	0.9	CW	6	1	PBM at 6h improved clinical rating score, except at the CW setting
								PW 1kHz			
								PW 100Hz			
Lapchak 2010[20]	Rabbit	RSCEM	Molecular	808nm	7.5	2	0.9	CW	.08 (5min)	1	Increased cortical ATP content compared to sham (41% for setting 1, 157% for setting 2, 221% for setting 3), CW increase was not statistically significant, measured 3h post-stroke
					37.5		4.5	PW 100Hz, 3.5mJ/ pulse			
					262.5		31.5	PW 100Hz, 24.5mJ/ pulse			
Uozomi 2010[30]	Mouse	Healthy	CBF (Laser Doppler), Histological	808nm Laser	560	45	1512*	CW	NA	1	Relative increase in CBF (measured by laser doppler flowmetry), increased NO
					1100		2970*				
					2200		5940*				
		BCCAO			1100	30	2970	CW	-30	1	
Yip 2011[15]	Rat	MCAO (transient, 1hr)	Molecular	660nm Laser		1	2.64	PW 10kHz	0	1	Increased anti-apoptotic factors (Akt, pAkt, pBAD, Bcl-2), decreased pro-aptotic factors (caspase 9, caspase 3)
						5	13.2				
						10	26.4				

Huisa 2013[36]	Rabbit	RSCEM	Behavioral	808nm Laser	7.5 10.8	2	0.9* 1.296*	CW	3 2	1	10.8mW/cm^2 improved clinical rating score
					7.5 20	2	0.9* 2.4*	CW	3 2	2 3	Improved clinical rating score, triple treatment best (69%, 265%)
Meyer 2016[37]	Rabbit	RSCEM	Behavioral	808nm Laser	7.5 55.6 111	2	0.9	CW PW 10Hz PW 100Hz	2	1	Improved clinical rating score, 100Hz setting showed largest improved
					55.6 111 333	2		PW 100Hz	2	3 3 3	Triple treatment imp roved clinical rating score, 333mW/cm^2 not effective
Lapchak 2016[38]	Rabbit	RSCEM	Behavioral, molecular	808nm Laser	7.5	2	0.9	CW	1	1	Improved clinical rating score, increased ATP
Yang 2018[39]	Rat	Photothro-Mbosis	Behavioral, molecular	808nm Laser	25	2	0.9	CW	24	7	Decreased behavioral deficits and infarct volume, stimulated neurogenesis, anti-inflammatory cytokines, CCO activity, ATP production
Tucker 2018[40]	Rat	Hypoxia-ischemia	Histological, molecular	808nm Laser	25	2	3	CW	24	7	Reduced brain lesion, mitochondrial fragmentation, pro-apoptotic factors, increased ATP
Wang 2019[41]	Rat	Global Cerebral Ischemia	Behavioral, histological	808nm Laser	8			CW	6	1 2 3 4	Improved short and long term behavioral deficits, decreased mitochondrial fragmentation
Salehpour 2019[41]	Mouse	BCCAO (transient, 20min)	Behavioral, molecular	810nm Laser				PW 10Hz		1	Improved cognition, lowered ROS, increased ATP, and mitochondrial activity
Fonseca 2019[42]	Rat	Ischemic stroke	Behavioral, structural	904nm LED		1.05	7	CW		3 7 21	Improved behavior, increased neurogenesis, reduced edema
Argibay 2019[43]	Rat	MCAO (transient, 60 min)	fMRI, structural	830nm LED	0.16*	30	0.28	CW	24	12 36	No recovery of BOLD signal, no reduction of lesion size, no evidence of neurogenesis

References

Argibay, B., Campos, F., Perez-Mato, M., Vieites-Prado, A., Correa-Paz, C., López-Arias, E., Da Silva-Candal, A., Moreno, V., Montero, C., Sobrino, T., Castillo, J., & Iglesias-Rey, R. (2019). Light-Emitting Diode Photobiomodulation After Cerebral Ischemia. *Frontiers in Neurology*, *10*.

Ball, K. A., Castello, P. R., & Poyton, R. O. (2011). Low intensity light stimulates nitrite-dependent nitric oxide synthesis but not oxygen consumption by cytochrome c oxidase: Implications for phototherapy. *Journal of Photochemistry and Photobiology B: Biology*, *102*(3), 182–191.

Chen, A. C. H., Arany, P. R., Huang, Y. Y., Tomkinson, E. M., Sharma, S. K., Kharkwal, G. B., Saleem, T., Mooney, D., Yull, F. E., Blackwell, T. S., & Hamblin, M. R. (2011). Low-Level Laser Therapy Activates NF-kB via Generation of Reactive Oxygen Species in Mouse Embryonic Fibroblasts. *PLoS ONE*, *6*(7), e22453.

Chow, R. T., Heller, G. Z., & Barnsley, L. (2006). The effect of 300 mW, 830 nm laser on chronic neck pain: A double-blind, randomized, placebo-controlled study. *Pain*, *124*(1), 201–210.

Chow R.T., Johnson M.I., Lopes-Martins R.A., Bjordal J.M. (2010). Efficacy of low-level laser therapy in the management of neck pain: a systematic review and meta-analysis of randomised placebo or active-treatment controlled trials. *The Spine Journal*, *10*(5), 456.

Chung, H., Dai, T., Sharma, S. K., Huang, Y. Y., Carroll, J. D., & Hamblin, M. R. (2012). The nuts and bolts of low-level laser (light) therapy. *Annals of biomedical engineering*, *40*(2), 516–533.

de Freitas, L. F., & Hamblin, M. R. (2016). Proposed Mechanisms of Photobiomodulation or Low-Level Light Therapy. *IEEE Journal of Selected Topics in Quantum Electronics*, *22*(3), 348–364.

de Jesus Fonseca, E. G., Pedroso, A., Neuls, D., Barbosa, D., Cidral-Filho, F. J., Salgado, A. S. I., Dubiela, A., Carraro, E., & Kerppers, I. I. (2019). Study of transcranial therapy 904 nm in experimental model of stroke. *Lasers in Medical Science*, *34*(8), 1619–1625.

de Lima, F. M., Moreira, L. M., Villaverde, A. B., Albertini, R., Castro-Faria-Neto, H. C., & Aimbire, F. (2010). Low-level laser therapy (LLLT) acts as cAMP-elevating agent in acute respiratory distress syndrome. *Lasers in Medical Science*, *26*(3), 389–400.

DeTaboada, L., Ilic, S., Leichliter-Martha, S., Oron, U., Oron, A., & Streeter, J. (2006). Transcranial application of low-energy laser irradiation improves neurological deficits in rats following acute stroke. *Lasers in Surgery and Medicine*, *38*(1), 70–73.

DeTaboada L, Yu J, El-Amouri S, Gattoni-Celli S, Richieri S, McCarthy T, Streeter J, Kindy MS. (2011). Transcranial laser therapy attenuates amyloid-β peptide neuropathology in amyloid-β protein precursor transgenic mice. *Journal of Alzheimer's Disease, 23*(3), 521-35.

Frangez, I., Cankar, K., Ban Frangez, H., & Smrke, D. M. (2017). The effect of LED on blood microcirculation during chronic wound healing in diabetic and non-diabetic patients—a prospective, double-blind randomized study. *Lasers in Medical Science*, *32*(4), 887–894.

Hacke, W., Schellinger, P. D., Albers, G. W., Bornstein, N. M., Dahlof, B. L., Fulton, R., Kasner, S. E., Shuaib, A., Richieri, S. P., Dilly, S. G., Zivin, J., Lees, K. R., & NEST 3 Committees and Investigators (2014). Transcranial laser therapy in acute stroke treatment: results of neurothera effectiveness and safety trial 3, a phase III clinical end point device trial. *Stroke*, *45*(11), 3187–3193.

Hamblin, M. R., & Huang, Y. (2019). Mechanisms of photobiomodulation in the brain. In *Photobiomodulation in the Brain: Low-Level Laser (Light) Therapy in Neurology and Neuroscience* (1st ed., pp. 97–110). Academic Press.

Hipskind, S. G., Grover, F. L., Fort, T. R., Helffenstein, D., Burke, T. J., Quint, S. A., Bussiere, G., Stone, M., & Hurtado, T. (2019). Pulsed Transcranial Red/Near-Infrared Light Therapy Using Light-Emitting Diodes Improves Cerebral Blood Flow and Cognitive Function in Veterans with Chronic Traumatic Brain Injury: A Case Series. *Photomedicine and Laser Surgery*, *37*(2), 77–84.

Huisa, B. N., Chen, Y., Meyer, B. C., Tafreshi, G. M., & Zivin, J. A. (2013). Incremental treatments with laser therapy augments good behavioral outcome in the rabbit small clot embolic stroke model. *Lasers in Medical Science*, *28*(4), 1085–1089.

Ivandic, B. T., & Ivandic, T. (2008). Low-Level Laser Therapy Improves Vision in Patients with Age-Related Macular Degeneration. *Photomedicine and Laser Surgery*, *26*(3), 241–245.

Karu, T. I., & Kolyakov, S. F. (2005). Exact Action Spectra for Cellular Responses Relevant to Phototherapy. *Photomedicine and Laser Surgery*, *23*(4), 355–361.

Kovacs, I. B., Mester, E., & Görög, P. (1974). Stimulation of wound healing with laser beam in the rat. *Experientia*, *30*(11), 1275–1276.

Lampl, Y., Zivin, J. A., Fisher, M., Lew, R., Welin, L., Dahlof, B., Borenstein, P., Andersson, B., Perez, J., Caparo, C., Ilic, S., & Oron, U. (2007). Infrared Laser Therapy for Ischemic Stroke: A New Treatment Strategy. *Stroke*, *38*(6), 1843–1849.

Lapchak, P. A., & Boitano, P. D. (2016). A novel method to promote behavioral improvement and enhance mitochondrial function following an embolic stroke. *Brain Research*, *1646*, 125–131.

Lapchak, P. A., & De Taboada, L. (2010). Transcranial near infrared laser treatment (NILT) increases cortical adenosine-5′-triphosphate (ATP) content following embolic strokes in rabbits. *Brain Research*, *1306*, 100–105.

Lapchak, P. A., Salgado, K. F., Chao, C. H., & Zivin, J. A. (2007). Transcranial near-infrared light therapy improves motor function following embolic strokes in rabbits: An extended therapeutic window study using continuous and pulse frequency delivery modes. *Neuroscience*, *148*(4), 907–914.

Lapchak, P. A., Wei, J., & Zivin, J. A. (2004). Transcranial Infrared Laser Therapy Improves Clinical Rating Scores After Embolic Strokes in Rabbits. *Stroke*, *35*(8), 1985–1988.

Lee, H. I., Park, J. H., Park, M. Y., Kim, N. G., Park, K.-J., Choi, B. T., Shin, Y.-I. I., & Shin, H. K. (2016). Pre-conditioning with transcranial low-level light therapy reduces neuroinflammation and protects blood-brain barrier after focal cerebral ischemia in mice. *Restorative Neurology and Neuroscience*, *34*(2), 201–214.

Leung, M. C. P., Lo, S. C. L., Siu, F. K. W., & So, K.-F. (2002). Treatment of experimentally induced transient cerebral ischemia with low energy laser inhibits nitric oxide synthase activity and up-regulates the expression of transforming growth factor-beta 1. *Lasers in Surgery and Medicine*, *31*(4), 283–288.

Mester, E., Szende, B., & Gärtner, P. (1968). The effect of laser beams on the growth of hair in mice. *Radiobiologia. Radiotherapia. (Berl.)*, *9*(5), 621-626.

Meyer, D. M., Chen, Y. M., & Zivin, J. A. (2016). Dose-finding study of phototherapy on stroke outcome in a rabbit model of ischemic stroke. *Neuroscience Letters*, *630*, 254–258.

Minatel, D. G., Frade, M. A. C., França, S. C., & Enwemeka, C. S. (2009). Phototherapy promotes healing of chronic diabetic leg ulcers that failed to respond to other therapies. *Lasers in Surgery and Medicine*, *41*(6), 433–441.

Naeser MA, Saltmarche A, Krengel MH, Hamblin MR, Knight JA. (2011). Improved cognitive function after transcranial, light-emitting diode treatments in chronic, traumatic brain injury: two case reports. *Photomedicine and Laser Surg*ery May; *29*(5):351-8.

Nejatifard, M., Asefi, S., Jamali, R., Hamblin, M. R., & Fekrazad, R. (2021). Probable positive effects of the photobiomodulation as an adjunctive treatment in COVID-19: A systematic review. *Cytokine*, *137*, 155312.

Oron, A., Oron, U., Chen, J., Eilam, A., Zhang, C., Sadeh, M., Lampl, Y., Streeter, J., DeTaboada, L., & Chopp, M. (2006). Low-Level Laser Therapy Applied Transcranially to Rats After Induction of Stroke Significantly Reduces Long-Term Neurological Deficits. *Stroke*, *37*(10), 2620–2624.

Oron A, Oron U, Streeter J, de Taboada L, Alexandrovich A, Trembovler V, Shohami E. (2007). Low-level laser therapy applied transcranially to mice following traumatic brain injury significantly reduces long-term neurological deficits. *Journal of Neurotrauma.* Apr; *24*(4):651-6.

Podogrodzki, J., Lebiedowski, M., Szalecki, M., Kępa, I., Syczewska, M., & Jóźwiak, S. (2016). Wpływ niskoenergetycznej laseroterapiina skorny przepływ krwi [Impact of low level laser therapy on skin blood flow]. *Developmental Period Medicine*, *20*(1), 40–46.

Salehpour F, Farajdokht F, Mahmoudi J, Erfani M, Farhoudi M, Karimi P, Rasta SH, Sadigh-Eteghad S, Hamblin MR and Gjedde A (2019) Photobiomodulation and Coenzyme Q10 Treatments Attenuate Cognitive Impairment Associated With Model of Transient Global Brain Ischemia in Artificially Aged Mice. *Frontiers in Cellular Neuroscience.* 13:74.

Salehpour, F., Mahmoudi, J., Kamari, F., Sadigh-Eteghad, S., Rasta, S. H., & Hamblin, M. R. (2018). Brain Photobiomodulation Therapy: a Narrative Review. *Molecular Neurobiology*, *55*(8), 6601–6636.

Salgado, A. S. I., Zângaro, R. A., Parreira, R. B., & Kerppers, I. I. (2014). The effects of transcranial LED therapy (TCLT) on cerebral blood flow in the elderly women. *Lasers in Medical Science*, *30*(1), 339–346.

Schubert, V. (2001). Effects of phototherapy on pressure ulcer healing in elderly patients after a falling trauma. A prospective, randomized, controlled study. *Photodermatology, Photoimmunology and Photomedicine*, *17*(1), 32–38.

Sharma SK, Kharkwal GB, Sajo M, Huang YY, De Taboada L, McCarthy T, Hamblin MR. (2011). Dose response effects of 810 nm laser light on mouse primary cortical neurons. *Lasers in Surgery and Medicine.* Sep; *43*(8):851-9.

Srinivasan, V. J., Sakadžić, S., Gorczynska, I., Ruvinskaya, S., Wu, W., Fujimoto, J. G., & Boas, D. A. (2010). Quantitative cerebral blood flow with Optical Coherence Tomography. *Optics Express*, *18*(3), 2477.

Sweeney, M. D., Kisler, K., Montagne, A., Toga, A. W., & Zlokovic, B. V. (2018). The role of brain vasculature in neurodegenerative disorders. *Nature Neuroscience*, *21*(10), 1318–1331.

Tucker, L. D., Lu, Y., Dong, Y., Yang, L., Li, Y., Zhao, N., & Zhang, Q. (2018). Photobiomodulation Therapy Attenuates Hypoxic-Ischemic Injury in a Neonatal Rat Model. *Journal of Molecular Neuroscience*, *65*(4), 514–526.

Uozumi, Y., Nawashiro, H., Sato, S., Kawauchi, S., Shima, K., & Kikuchi, M. (2010). Targeted increase in cerebral blood flow by transcranial near-infrared laser irradiation. *Lasers in Surgery and Medicine*, *42*(6), 566–576.

Wang, X., Tian, F., Soni, S., Gonzalez-Lima, F., Liu, Hanli. (2016). Interplay between up-regulation of cytochrome-c-oxidase and hemoglobin oxygenation induced by near-infrared laser. *Scientific Reports* **6,** 30540.

Yang, L., Tucker, D., Dong, Y., Wu, C., Lu, Y., Li, Y., Zhang, J., Liu, T. C.-Y., & Zhang, Q. (2018). Photobiomodulation therapy promotes neurogenesis by improving post-stroke local microenvironment and stimulating neuroprogenitor cells. *Experimental Neurology*, *299*, 86–96.

Yip, K. K., Lo, S. C., Leung, M. C., So, K. F., Tang, C. Y., & Poon, D. M. (2011). The effect of low-energy laser irradiation on apoptotic factors following experimentally induced transient cerebral ischemia. *Neuroscience*, *190*, 301–306.

Zein, R., Selting, W., & Hamblin, M. R. (2018). Review of light parameters and photobiomodulation efficacy: dive into complexity. *Journal of Biomedical Optics*, *23*(12), 1.

Zivin, J. A., Albers, G. W., Bornstein, N., Chippendale, T., Dahlof, B., Devlin, T., Fisher, M., Hacke, W., Holt, W., Ilic, S., Kasner, S., Lew, R., Nash, M., Perez, J., Rymer, M., Schellinger, P., Schneider, D., Schwab, S., Veltkamp, R., … Streeter, J. (2009). Effectiveness and Safety of Transcranial Laser Therapy for Acute Ischemic Stroke. *Stroke*, *40*(4), 1359–1364.

CURRICULUM VITAE